COMMUNICATION

Remote Electronic Effect on the N-Heterocyclic Carbene-catalyzed Asymmetric Intramolecular Stetter Reaction and Structural Revision of Products

Received 00th January 20xx,
Accepted 00th January 20xx

DOI: 10.1039/x0xx00000x

Tsubasa Inokuma,[a,b] Kohei Iritani,[a] Yuki Takahara,[a] Chunzhao Sun,[a] Yousuke Yamaoka,[c] Satoru Kuwano[c] and Ken-ichi Yamada*[a,b]

The remote electronic effects of chiral N-heterocyclic carbene catalysts on the asymmetric intramolecular Stetter reaction are investigated. The reaction rate and enantioselectivity were markedly influenced by a substituent at a remote position of the catalyst. The absolute configurations of the products are revised by X-ray diffraction. Density-functional theory calculations rationalize the improvement of the enantioselectivity using an electron-deficient catalyst.

The hydroacylation of an activated olefin by an aldehyde catalyzed by cyanide or an N-heterocyclic carbene (NHC), the so-called Stetter reaction, is a representative reaction involving the Umpolung of aldehydes.[1,2] After the first asymmetric intramolecular Stetter reaction was accomplished using a chiral NHC by Enders et al. in 1996,[3] this reaction has been established as a benchmark reaction for the study of newly developed chiral NHCs.[4–10] In an addition to the effort for improving the yield and enantioselectivity, a mechanistic study has been also of interest. The mechanism depicted in Scheme 1 has been previously proposed.[11] The reaction starts with the addition of an NHC to an aldehyde to form tetrahedral intermediate **I**, which undergoes tautomerization to the so-called Breslow intermediate **II** (Scheme 1). An intramolecular conjugate addition follows to produce enolate intermediate **III**, which tautomerizes to alkoxide intermediate **IV**. Subsequent elimination of the NHC releases the product and regenerates the NHC catalyst. Rovis et al. reported that the proton transfer to form **II** is the first irreversible step[12] and that the addition of catechol enhances the rate of the Stetter-type reaction of enals and nitroalkenes probably due to an acceleration of the proton transfer step.[13] Smith et al. reported that an electron-deficient *N*-aryl substituent of triazolylidene-type NHC accelerated the intramolecular Stetter reaction, probably due to the increased acidity of the transferred proton in the intermediate **I,** to facilitate the rate-determining proton transfer.[14] Density-functional theory (DFT) calculations reported by Domingo et al. showed that the activation energy of the proton transfer step is higher than that of the other reaction steps, which allowed them to conclude that the proton transfer is the rate-determining step.[15]

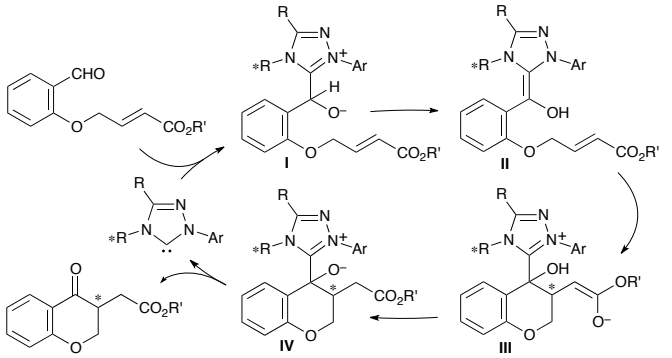

Scheme 1. Proposed Mechanism of the Intramolecular Stetter Reaction.

During our research on organocatalyzed reactions,[16–23] we achieved the electronic tuning of an aminoindanol-derived chiral NHC[24] by installing a remote electron-withdrawing substituent.[25] Although substitution of the N-aryl group of NHCs is a common strategy to tune the catalyst efficiency,[14,26–28] the remote substitution provided a much more effective improvement of the rate and the enantioselectivity during the acylative kinetic resolution of diols and hydroxy thioamides probably because the substituents are located far from the carbene carbon atom, causing less steric or electrostatic interference in the reaction.[29,30] Having achieved the remote electronic tuning of NHCs, we were interested in applying it to the Stetter reaction. We envisaged that the use of an electron-deficient NHC could accelerate the Stetter reaction if the

[a] Graduate School of Pharmaceutical Sciences, Tokushima University, Shomachi, Tokushima 770-8505, Japan.
[b] Research Cluster on "Key Material Development", Tokushima University, Shomachi, Tokushima 770-8505, Japan.
[c] Graduate School of Pharmaceutical Sciences, Kyoto University, Yoshida, Sakyo-ku, Kyoto 606-8501, Japan.

† Electronic Supplementary Information (ESI) available: [details of any supplementary information available should be included here]. See DOI: 10.1039/x0xx00000x

remote electronic effect is operative and increases the acidity of the hydrogen atom that is to be transferred in tetrahedral intermediate **I** because the proton transfer is a rate-determining step. Herein, we report the electronic effects of an NHC catalyst on the asymmetric intramolecular Stetter reaction and the structural revision of the products.

We started our investigation on the remote electronic effect using triazolium salt **1a** as a catalyst precursor and salicylaldehyde-derived alkenoate **2a** as a substrate (Table 1). A mixture of **1a** and 1,8-bis(dimethylamino)naphthalene (proton sponge) (1 mol% each) in dichloroethane was stirred at room temperature for 1 h to generate the corresponding NHC, and **2a** was then added to the mixture at 0 °C. After 100 min, γ-keto ester **3a** was produced in 53% yield with 96% ee and $[\alpha]_D$[19] of –9.4 (*c* 1.1, $CHCl_3$) (entry 2). Although the absolute configuration of **3a** having $[\alpha]_D$ of –4.6 (*c* 1.0, $CHCl_3$) was previously assigned as *R*,[3] an X-ray diffraction study revealed that **3a** possesses an *S* configuration (*vide infra*). As expected, the reaction with **1c** bearing an electron-donating group became slower to give **3a** in 50% yield (entry 1). In contrast, the reactions with an electron-deficient NHC derived from bromo-containing **1b** proceeded much faster, giving **3a** in 73% yield with 97% ee (entry 3). The use of more electron-deficient NHCs, such as those derived from **1d** and **1e,** significantly accelerated the reaction, which produced **3a** in 85% and 89% yields, respectively (entries 4 and 5). Interestingly, the remote substituents also affected the enantioselectivity; the product was obtained with higher enantiomeric excess as the electron-withdrawing character of the substituent increased more (entries 1–5).

Table 1 Asymmetric Intramolecular Stetter Reaction of **2a** Using **1a–e**.[a]

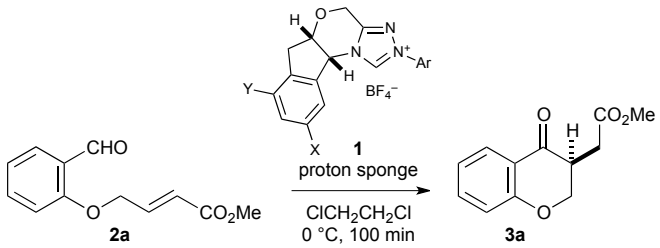

entry	**1**	X	Y	% yield	% ee
1	**1c**[b]	Me	H	50	92[c]
2	**1a**	H	H	53	96
3	**1b**[b]	Br	H	73	97[c]
4	**1d**[b]	NO_2	H	85	98[c]
5	**1e**	NO_2	Br	89	98

[a] The reactions were performed using 1 mol% each of **1** and proton sponge. [b] Antipode was used. [c] Antipode was obtained.

Next, we investigated the reaction of β-disubstituted alkenoate **2b** (Table 2) because the absence of an α-proton in the product excludes the possibility of decreasing the enantiomeric excess by the α-deprotonation.[31–34] The reaction of **2b** was much slower than that of **2a** and therefore was performed at 40 °C using 20 mol% catalysts. The reaction rate increased as the electron-withdrawing ability of the NHC substituent increased, giving **3b** in 44%, 52%, 70%, and 77% yield when the substituent X was Me, H, Br, and NO_2, respectively (entries 1–4). When the most electron-deficient NHC derived from **1e** (X = NO_2, Y = Br) was used, the reaction was further accelerated, and **3b** was obtained in 83% yield (entry 5). The use of electron-deficient NHCs increased the enantioselectivity also in the reaction of **2b** (entries 1–5).

Table 2 Asymmetric Intramolecular Stetter Reaction of **2b** Using **1a–e**.[a]

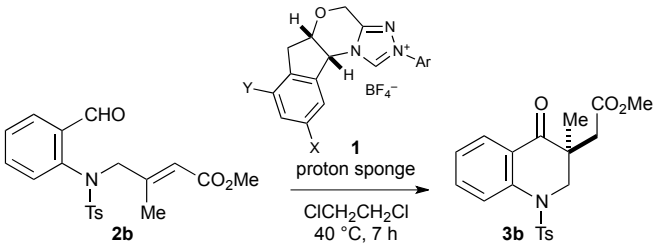

entry	**1**	X	Y	% yield	% ee
1	**1c**[b]	Me	H	44	74[c]
2	**1a**	H	H	52	78
3	**1b**[b]	Br	H	70	86[c]
4	**1d**[b]	NO_2	H	77	92[c]
5	**1e**[b]	NO_2	Br	83	95[c]

[a] The reactions were performed using 20 mol% each of **1** and proton sponge. [b] Antipode was used. [c] Antipode was obtained.

As the rate-determining step of the reaction is the proton transfer of tetrahedral intermediate **I** to form Breslow intermediate **II**, the above results indicate that the hydrogen atom to be transferred becomes more acidic as the substituents of the indane moiety of NHC become electron-withdrawing. This provides an additional example of the remote electronic effect of NHC, which we previously reported in the asymmetric acylation reactions.[25,29,30]

The absolute configuration of **3a** and **3b** was determined by X-ray diffraction analysis. To this aim, **3a** was reduced with sodium borohydride, followed by treatment with a catalytic amount of *p*-toluenesulfonic acid to give *cis*-lactone **4** and *trans*-alcohol **5** in 39% and 51% yield, respectively (Scheme 2).[35–37] Then, condensation of alcohol **5** with camphor derivative **6**[38–44] provided **7** in 75% yield.

Recrystallization of **7** from ethyl acetate/hexane provided a single crystal suitable for X-ray diffraction, which revealed the *S* configuration at the stereogenic center of **3a**. Meanwhile, recrystallization of **3b**[45] from isopropanol/hexane afforded a single crystal of **3b**, whose absolute configuration was also determined to be *S* by X-ray diffraction.[46] These results confirm that the reactions of **2a** and **2b** proceed with the same sense of stereoinduction.

The absolute configuration of **3a** was previously assigned to be *R* on the basis of Mosher's method.[3] In that work, the pyranone moiety was reduced to the corresponding *cis*-alcohol, which was subsequently converted to the corresponding Mosher ester with α-methoxy-α-(trifluoromethyl)phenylacetyl (MTPA) chloride. The absolute configuration of the stereogenic center formed during the Stetter reaction was then assigned according to the chemical-shift nonequivalences caused by the diatropic ring current of the phenyl ring in the MTPA ester.

However, as shown in Scheme 2 and previous reports,[35–37] the *cis*-alcohol produced by the reduction of 4-chromanone-2-acetate is unstable and prone to form *cis*-lactone. Therefore, the alcohol converted into the Mosher ester was most likely *trans*- instead of *cis*-configurated, which would explain the misassignment.

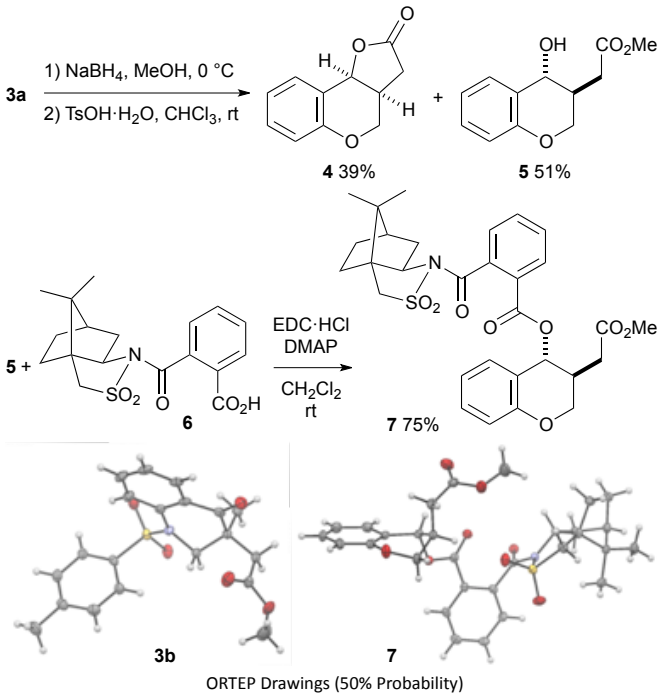

Scheme 2. Conversion of **3a** into **7** and ORTEP Drawings of **3b** and **7**.

To obtain insight into the increased enantioselectivity induced by electron-deficient NHCs, we performed DFT calculations of the transition-state geometries of the C–C bond-formation step at the B3LYP/6-31G* theoretical level (Figure 1). In the optimal transition-state geometries to give **3a** and its enantiomer *ent*-**3a**, the bond formation occurs on the *re*-face of the Breslow intermediate with the alkenoate moiety in an *s-cis*-conformation. In the transition state to give *ent*-**3a**, the developing negative charge in the alkenoate moiety is stabilized by the formation of a hydrogen bond between the ester carbonyl oxygen and the hydroxy group of the Breslow intermediate (red dash line). Meanwhile, in the transition state to give **3a**, the developing negative charge is doubly stabilized by a hydrogen bond between the ester α-carbon and the hydroxy group (blue dash line) and by an electrostatic interaction between the ester carbonyl oxygen and the benzylic hydrogen of the indane moiety (magenta dash line). The noncovalent interaction analysis[47] also supported the existence of these attractive interactions (see SI). The distance between the ester carbonyl oxygen and the indane benzylic hydrogen decreases as the electron-withdrawing character of the substituents of the indane benzene ring increases (i.e., 2.080, 2.065, and 2.032 Å in the transition state derived from **1c**, **1a**, and **1d**, respectively), which suggests that the remote electron-withdrawing substituents enhance the enantioselectivity through this additional interaction. Indeed, the natural charges of the benzylic hydrogen atoms were +0.272, +0.273, and +0.277 in NHC derived from **1c**, **1a**, and **1d**, respectively, at the B3LYP/6-31G* theoretical level. The positive charge and thus hydrogen-bonding ability increased as the substituent of NHCs became more electron-withdrawing. The free-energy difference between the major and minor transition states derived from **1c**, **1a**, and **1d** was determined to be 1.92, 2.18, and 2.49 kcal/mol at the B3LYP-D3/6-311+G(2df,2p)//B3LYP/6-31G* theoretical level, corresponding to 92%, 95%, and 97% ee, respectively, which are in good agreement with the experimental results (Table 1) and therefore, strongly indicate that the C–C bond-formation is probably the enantio-determining step.

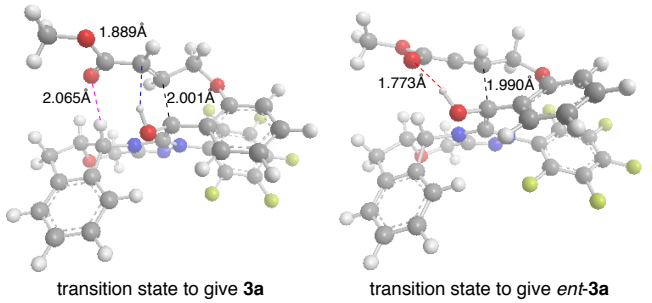

Fig. 1. Chem3D Perspective View of DFT Transition State Geometries to Give **3a** with **1a**.

To further demonstrate the practicality of the remote electronic tuning of the NHC, we applied it to the Stetter reaction of **2c** to give benzofuranone **3c**, which is challenging because **3c** tends to undergo base-induced racemization, limiting to 30% ee the best enantiomeric excess achieved to date (Scheme 3).[24,48–49] We expected that the less basic NHC derived from **1e** could minimalize the undesired racemization of the product. As expected, the reaction using *ent*-**1e**, which reached completion after 2 h, produced *ent*-**3c** quantitatively with 91% ee, whereas the use of **1a** afforded **3c** quantitatively with 84% ee after 2 h.

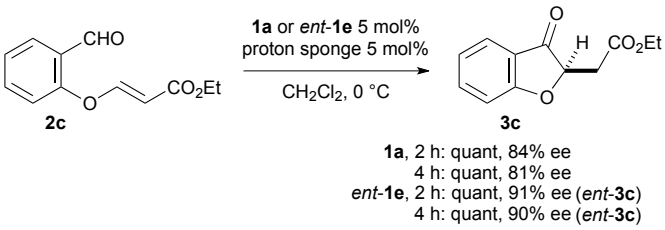

Scheme 3. Reaction of **2c** Using NHCs **1a** and *ent*-**1e**.

When the reaction was not quenched immediately after the completion of the reaction with **1a**, the enantiomeric excess of **3c** decreased to 81% ee, which clearly shows that the racemization of **3c** occurs under the reaction conditions. Conversely, in the reaction with *ent*-**1e**, the racemization was considerably retarded, and *ent*-**3c** was obtained with 90% ee after 4 h.

In summary, the Stetter reaction was investigated by using NHCs electronically tuned via remote substituents. The

reaction became fast as the substituents of NHC became more electron-withdrawing. This result is consistent with the two conclusions that the rate-determining step is the proton transfer to give the Breslow intermediate as previously reported,[12–15] and that the remote electronic effect is operative as we previously proposed.[25,29,30] The enantioselectivity increased when an electron-deficient NHC was used as a catalyst, which stabilized the major transition state probably by hydrogen-bonding. Furthermore, the use of NHCs bearing remote electron-withdrawing groups helps avoiding base-induced racemization of easily deprotonatable products. The absolute configuration of the product was determined by X-ray diffraction analysis, which led to the structural revision of **3a** as well as many other related compounds, whose absolute configuration had been assigned by analogy to **3a**.[50] Due to the misassignment, the result of DFT calculations has been puzzling; that is, a transition state of the lowest energy gives the commonly believed minor enantiomer. However, the structural revision solved this problem and enabled DFT calculations to rationalize the enantioselectivity.

We thank Kentaro Hashimoto and Yuna Watanabe for their contribution to the preliminary stage, and JSPS (KAKENHI JP22H05569), the Mochida Memorial Foundation for Medical and Pharmaceutical Research, Tokushima University (Research Clusters program No. 2201004), and the Japan Science Society (Sasakawa Scientific Research Grant) for financial support. C.S. thanks scholarship from JST (JPMJSP2113).

Conflicts of interest

There are no conflicts to declare.

Notes and references

1 H. Stetter, M. Schreckenberg, *Angew. Chem., Int. Ed.*, 1973, **12**, 81.
2 H. Stetter, H. Kuhlmann, *Synthesis*, 1975, **1975**, 379.
3 D. Enders, K. Breuer, J. Runsink, J. H. Teles, *Helv. Chim. Acta.*, 1996, **79**, 1899.
4 D. Ragno, G. Di Carmine, A. Brandolese, O. Bortolini, P. P. Giovannini, A. Massi, *ACS Catal.*, 2017, **7**, 6365.
5 K. E. Ozboya, T. Rovis, *Synlett*, 2014, **25**, 2665.
6 Y. Bao, N. Kumagai, M. Shibasaki, *Tetrahedron: Asymmetry*, 2014, **25**, 1401.
7 T. Soeta, Y. Tabatake, Y. Ukaji, *Tetrahedron*, 2012, **68**, 10188.
8 M.-Q. Jia, Y. Li, Z.-Q. Rong, S.-L. You, *Org. Biomol. Chem.* 2011, **9**, 2072.
9 J. R. Struble, J. Kaeobamrung, J. W. Bode, *Org. Lett.*, 2008, **10**, 957.
10 J. Pesch, K. Harms, T. Bach, *Eur. J. Org. Chem*., 2004, 2025.
11 H. Stetter, *Angew. Chem., Int. Ed. Engl.*, 1976, **15**, 639.
12 J. L. Moore, A. P. Silvestri, J. Read de Alaniz, D. A. DiRocco, T. Rovis, *Org. Lett.*, 2011, **13**, 1742.
13 D. A. DiRocco, T. Rovis, *J. Am. Chem. Soc.*, 2011, **133**, 10402.
14 C. J. Collett, R. S. Massey, O. R. Maguire, A. S. Batsanov, A.M. C. O'Donoghue, A. D. Smith, *Chem. Sci.*, 2013, **4**, 1514.
15 L. R. Domingo, R. J. Zaragozá, J. A. Saéz, M. Arnó, *Molecules*, 2012, **17**, 1335.
16 Inokuma, T.; Masui, K.; Fukuhara, K.; Yamada, K. *Chem. Eur. J.* 2023, **29**, e202203120.
17 K. Yamasaki, A. Yamauchi, T. Inokuma, Y. Miyakawa, Y. Wang, R. Oriez, Y. Yamaoka, K. Takasu, N. Tanaka, Y. Kashiwada, K. Yamada, *Asian J. Org. Chem.,* 2021, **10**, 1828.
18 T. Jichu, T. Inokuma, K. Aihara, T. Kohiki, K. Nishida, A. Shigenaga, K. Yamada, A. Otaka, *ChemCatChem*, 2018, **10**, 3402.
19 B. Kang, Y. Wang, S. Kuwano, Y. Yamaoka, K, Takasu, K. Yamada, *Chem. Commun.*, 2017, **53**, 4469.
20 Y. Wang, R. Oriez, S. Oh, Y. Miyakawa, Y. Yamaoka, K, Takasu, K. Yamada, *Heterocycles*, 2017, **95**, 413.
21 Y. Wang, R. Oriez, S. Kuwano, Y. Yamaoka, K. Takasu, K. Yamada, *J. Org. Chem*., 2016, **81**, 2652.
22 B. Kang, T. Sutou, Y. Wang, S. Kuwano, Y. Yamaoka, K. Takasu, K. Yamada, *Adv. Synth. Catal.*, 2015, **357**, 131.
23 S. Kuwano, S. Harada, R. Oriez, K. Yamada, *Chem. Commun.,* 2012, **48**, 145.
24 M. S. Kerr, J. Read de Alaniz, T. Rovis, *J. Am. Chem. Soc.*, 2002, **124**, 10298.
25 S. Kuwano, S. Harada, B. Kang, R. Oriez, Y. Yamaoka, K. Takasu, K. Yamada, *J. Am. Chem. Soc.*, 2013, **135**, 11485.
26 J. Read de Alaniz, T. Rovis, *J. Am. Chem. Soc.*, 2005, **127**, 6284.
27 H. Takikawa, K. Suzuki, *Org. Lett.*, 2007, **9**, 2713.
28 J. Mahatthananchai, J. W. Bode, *Chem. Sci.*, 2012, **3**, 192.
29 K. Yamada, A. Yamauchi, T. Fujiwara, K. Hashimoto, Y. Wang, S. Kuwano, T. Inokuma, *Asian J. Org. Chem.,* 2022, **11**, e202200452.
30 Y. Wang, A. Yamauchi, K. Hashimoto, T. Fujiwara, T. Inokuma, Y. Mitani, K. Ute, S. Kuwano, Y. Yamaoka, K. Takasu, K. Yamada, *ACS Catal.*, 2022, **12**, 6100.
31 A. Rafiński, A. Kozakiewicz, K. Rafińska, *ACS Catal.*, 2014, **4**, 1404.
32 J. L. Moore, M. S. Kerr, T. Rovis, *Tetrahedron*, 2006, **62**, 11477.
33 Z. Rafiński, *Catalysts*, 2019, **9**, 192.
34 K. Dzieszkowski, Z. Rafiński, *Adv. Synth. Catal.*, 2020, **362**, 3830.
35 J. Bentley, P. A. Nilsson, A. F. Parsons, *J. Chem. Soc., Perkin Trans. 1*, 2002, 1461.
36 C. D. Donner, M. I. Casana, *Tetrahedron Lett.*, 2012, **53**, 1105.
37 H. Santoso, M. I. Casanac, M. I. C. D. Donner, *Org. Biomol. Chem.*, 2014, **12**, 171.
38 S. Toyota, A. Yasutomi, M. Ōki, *Tetrahedron Lett.*, 1995, **36**, 6297
39 N. Harada, N. Koumura, B. L. Feringa, *J. Am. Chem. Soc.*, 1997, **119**, 7256.
40 S. Toyota, A. Yasutomi, H. Kojima, Y. Igarashi, M. Asakura, M. Ōki, *Bull Chem. Soc. Jpn*., 1998, **71**, 2715.
41 K. Tomooka, N. Komine, T. Sasaki, H. Shimizu, T. Nakai, *Tetrahedron Lett.*, 1998, **39**, 9715.
42 M. Watanabe, S. Kuwahara, N. Harada, M. Koizumi, T. Ohkuma, T. *Tetrahedron: Asymmetry*, 1999, **10**, 2075.
43 P. T. Le, S. J. Brickner, S. K. Wade, K. Brighty, R. Monahan, G. G. Stone, D. Girard, S. Finegan, J. Duignan, J. Schafer, M. Maloney, R. P. Zaniewski, A. G. Connolly, J. Liras, J. Bordner, I. Samardjiev, *Bioorg. Med. Chem. Lett.*, 2011, **21**, 276.
44 R. Ramesh, P. S. Swaroop, R. G. Gonnade, C. Thirupathi, R. A. Waterworth, J. G. Millar, D. S. Reddy, *J. Org. Chem.*, 2013, **78**, 6281.
45 Prepared by the reaction with **1d** (not *ent*-**1d**) as a catalyst; see the SI for more details.
46 Crystallographic data have been deposited with Cambridge Crystallographic Data Centre (CCDC-2208224 and 2208225).
47 E. R. Johnson, S. Keinan, P. Mori-Sánchez, J. Contreras-García, A. J. Cohen, W. Yang, *J. Am. Chem. Soc.*, 2010, **132**, 6498.
48 J. R. de Alaniz, M. S. Kerr, J. L. Moore, T. Rovis, *J. Org. Chem.*, 2008, **73**, 2033.
49 Z.-Q. Rong, Y. Li, G.-Q. Yang, S.-L. You, *Synlett*, 2011, 1033.
50 We found more than 80 compounds misassigned by analogy to **3a**.